Relativistic model for nuclear matter and atomic nuclei with momentum-dependent self-energies

S. Typel

Gesellschaft für Schwerionenforschung mbH (GSI),
Theorie, Planckstraße 1, D-64291 Darmstadt, Germany
(Dated: February 9, 2008)

The Lagrangian density of standard relativistic mean-field (RMF) models with density-dependent meson-nucleon coupling vertices is modified by introducing couplings of the meson fields to derivative nucleon densities. As a consequence, the nucleon self energies, that describe the effective in-medium interaction, become momentum dependent. In this approach it is possible to increase the effective (Landau) mass of the nucleons, that is related to the density of states at the Fermi energy, as compared to conventional relativistic models. At the same time the relativistic effective (Dirac) mass is kept small in order to obtain a realistic strength of the spin-orbit interaction. Additionally, the empirical Schrödinger-equivalent central optical potential from Dirac phenomenology is reasonably well described. A parametrization of the model is obtained by a fit to properties of doubly magic atomic nuclei. Results for symmetric nuclear matter, neutron matter and finite nuclei are discussed.

I. INTRODUCTION

The relativistic description of nuclear matter and atomic nuclei advanced considerably in recent years by improving the underlying density functional [1, 2, 3, 4]. Originally, these nuclear systems were treated in the language of a relativistic quantum field theory (Quantum Hadrodynamics) based on a relativistic Lagrangian density that contains nucleons and mesons as degrees of freedom. In recent years, the viewpoint has changed and the approach is considered as an effective field theory, see e.g. [5]. The model can be seen as a special variant of density functional theory [6] and a connection to the underlying theory of Quantum Chromodynamics was established [7].

In principle, it is possible to describe the ground state of nuclei exactly due to the Hohenberg-Kohn theorem [8] as soon as the correct functional of the local baryon density is known. Unfortunately, there is no explicit scheme for constructing such a functional. Nuclear theory is concerned to develop a sufficiently accurate approximation guided by experience and the physical knowledge of the system. Instead of using functionals based on the density alone, one can start from a functional that contains additional densities, e.g. the kinetic energy density. This approach automatically leads to the Kohn-Sham equations for the nucleons [9], i.e. a Schrödinger-type equation in the non-relativistic case and a Dirac-type equation in the relativistic case, respectively. In these equations the effective interaction is expressed by potentials or by self-energies, respectively, that depend non-trivially on the nucleon fields.

There is a big advantage of the Kohn-Sham approach since certain physical effects are more easily incorporated into the description. Functionals that are solely based on the density can be compared to a description of finite nuclei in a Thomas-Fermi approximation where no shell effects appear. Considering also the kinetic density in the functional, corresponding to a Hartree or Hartree-Fock description, shell effects emerge automatically. In non-relativistic approaches a spin current density is included in the functional to generate the large spin-orbit splittings observed in finite nuclei. These three densities in the non-relativistic framework are replaced by the baryon (or vector) density, the kinetic density and the scalar density in relativistic approaches. Pairing effects can be included by introducing the corresponding pairing densities. Additionally, in case of neutron-proton asymmetric systems, one has to deal with both isoscalar and isovector versions of these quantities.

A general functional can be constructed in terms of the considered densities and their derivatives. Due to the Lorentz structure and the isospin degree of freedom there is a large variety of possible contributions that can appear in a relativistic density functional and it is not clear what possible densities and combinations are really relevant in the description. The density functional can be expanded in powers of the nucleon field, the meson fields, and their derivatives. The importance of the individual contributions can be estimated in a systematic approach that is guided by the principles of naive dimensional analysis and of the naturalness of the appearing coupling constants [5, 10, 11]. It is also possible to compare with more fundamental approaches based on QCD and chiral symmetry. For large densities, however, this approach might be problematic due to the resulting polynomial dependence of the functional on the Fermi momentum or the density. Well-behaved rational approximations seem to be a promising alternative. Extrapolations to high densities are necessary in the application of the model, e.g. in the description of heavy-ion collisions or neutron stars.

The usual starting point in relativistic models is a certain Lagrangian density instead of an equivalent energy functional. This Lagrangian can be treated in different approximations. For a practical application to nuclear matter and finite nuclei one usually employs the mean-field approximation. In this approach the nucleon

self-energies in nucler matter become simple functions of various nucleon densities. In principle, one can go beyond the mean-field approximation in a quantum field theoretical treatment by a systematic diagrammatic expansion. In this case, the nucleon self-energies will have a much more complicated structure that takes the nontrivial effects of the nuclear medium into account. In Dirac Brueckner calculations of nuclear matter based on a given nucleon-nucleon interaction it is possible to extract the corresponding nucleon self energies, see, e.g., [12, 13, 14, 15, 16]. They show a dependence on both the density of the nuclear medium and the energy and momentum of the nucleon. An alternative approach to these "ab-initio" strategies for the nuclear many-body problem is a phenomenological treatment of the problem where the mean-field approximation is retained with its virtues in applying the model self-consistently to nuclear matter and finite nuclei with reasonable effort. However, the basic Lagrangian has to be modified for a quantitative description of the various properties and it becomes mandatory to introduce new terms or to modify existing contributions in the Lagrangian. The parameters of the model have to be fitted to properties of nuclear matter and atomic nuclei. They cannot be derived in a simple manner from a more basic description. In this work the phenomenological strategy is followed since it is known from experience that this approach is very successful. A selection of the relevant terms and of a more generalized functional form that is guided by other approaches, e.g. Dirac Brueckner calculations, and by physical intuition may lead to reasonable results.

In relativistic approaches to nuclear structure it is common to introduce meson fields as explicit degrees of freedom in the Lagrangian or density functional. In the modern point of view, they have to be seen as auxiliary fields that, a priori, have not to be identified with the corresponding mesons in free space although they share the same Lorentz and isospin structure. In principle, these fields can be completely removed from the theory as, e.g., in the relativistic point-coupling models [5, 10, 17, 18]. In the following, however, we will keep these meson fields in the model for convenience.

A quantitative description of nuclear systems was achieved by considering an explicit medium dependence of the effective interaction. For that purpose non-linear self-interactions of the mesons were introduced and the corresponding coupling constants were fitted to properties of nuclear matter and finite nuclei mostly close to the valley of stability, see e.g. [19, 20, 21, 22, 23, 24, 25, 26, 27, 28, 29, 30, 31, 32, 33, 34]. At large densities, however, this approach is not really reliable due to the polynomial dependence on the fields and instabilities can occur. Alternatively, a density dependence of the meson-nucleon couplings was considered [15, 34, 35, 36, 37, 38, 39, 40, 41, 42, 43]. In Ref. [40] it has been pointed out that, in general, the couplings have to be treated as functionals of the nucleon fields leading to rearrangement contributions to the self-energies that

are necessary for the thermodynamical consistency of the model. It is possible to choose functional forms (e.g. well-behaved rational functions) that are motivated by results of Dirac-Brueckner calculations of nuclear matter [15, 41]. This class of models seems to be the more flexible approach with proper high density behavior. Originally, the medium dependence was introduced only in the isoscalar part of the interaction. In recent years it was realized that it is also necessary to allow for a density dependence in the isovector channel in order to obtain a reasonable description of the neutron skin thickness of stable nuclei, the neutron matter equation of state and a reliable extrapolation to exotic nuclei [44, 45]. In all these standard relativistic approaches the self-energies in the Dirac equation for the nucleons depend nontrivially on the various densities. However, they are the same for all protons and neutrons, respectively, independent of the single-particle state.

Despite the success of the relativistic approach there are still some deficiencies that have to be dealt with in further extensions of the underlying density functional. The size of the scalar (Σ) and vector (Σ_μ) self-energies in the interior of a finite nucleus is well determined by requiring that the corresponding central and spin-orbit potentials have the correct strength. (For alternative definitions of the non-relativistic potential see, e.g., Ref. [48].) They are derived in a nonrelativistic reduction of the Dirac equation. The Schrödinger-equivalent central potential

$$V_{\text{cen}} = \frac{E}{m}\Sigma_0 - \Sigma + \frac{1}{2m}\left(\Sigma^2 - \Sigma_0^2\right) \qquad (1)$$

and the spin-orbit potential

$$V_{\text{so}} = \frac{\frac{d}{dr}\left(\Sigma_0 + \Sigma\right)}{E + m - \Sigma_0 - \Sigma}\frac{\vec{\sigma}\cdot\vec{L}}{2mr} \qquad (2)$$

of a nucleon with restmass m and energy E in a spherical nucleus are determined by the sum and the difference of the time component of the vector self-energy Σ_0 and the scalar self-energy Σ, fixing both quantities. Correspondingly, in symmetric nuclear matter at saturation density $\varrho_{\text{sat}} = 2k_F^3/(3\pi^2)$ with Fermi momentum $p_F = \hbar k_F$ the relativistic effective (Dirac) mass

$$m^* = m - \Sigma \qquad (3)$$

that is independent of the nucleon momentum and the chemical potential

$$\mu = \Sigma_0 + \sqrt{(m^*)^2 + p_F^2} \qquad (4)$$

are well determined.

In conventional RMF models the self-energies are independent of the nucleon energy and momentum but they exhibit a strong density dependence. However, from Dirac-Brueckner calculations one would expect that the self-energies also depend on the energy and momentum

of the nucleon in the medium. The central potential (1) allows to quantify this effect in both relativistic and non-relativistic models. Standard RMF models show a linear increase of the central potential. Only models with explicit energy or momentum dependent self-energies show a different result. In order to compare the energy or momentum dependence of (1) with empirical data it is common practice to compare the model predictions with the optical potential in nuclear matter extracted from Dirac phenomenology (DP) for elastic proton-nucleus scattering [46, 47]. In this approach scattering observables are fitted to experimental data up to approx. 1 GeV kinetic energy by varying the strength of the vector and scalar self-energies (real and imaginary part) of the target. The potential shape is described in simple parametrizations [46, 47] or taken from microscopic descriptions [48]. In DP the self-energies depend on the proton energy. The derived Schrödinger-equivalent central potential, extrapolated to nuclear matter, exhibits a non-linear energy dependence. At high energies a saturation of the optical potential with a value around 50 MeV is observed. (Imaginary contributions of the self-energies as extracted from Dirac phenomenology have an almost negligible influence on the real part of the corresponding optical potential. They enter only through the terms quadratic in the self-energies in Eq. (1). These contributions almost cancel each other since they are of similar magnitude.) At low kinetic energies, the optical potential is a nearly linear function of the energy. The self-energies in DP itself show an almost linear energy dependence for not too high energies. This observation and the experience from Dirac-Brueckner calculations motivates to consider a phenomenological extension of standard relativistic models that generates energy or momentum dependent self-energies already on the mean-field level.

Besides the relativistic effective (Dirac) mass m^* there are a number of other effective masses that have been introduced in the literature. For a general overview of definitions for effective masses in relativistic and non-relativistic calculations see [49]. An important quantity is the effective Landau mass

$$m_{\text{eff}} = p \frac{dp}{dE} \qquad (5)$$

that is related to the density of states $\varrho = m_{\text{eff}} p / (2\pi\hbar)^3$ in nuclear matter. The Landau mass is easily calculated from the dispersion relation

$$(E - \Sigma_0)^2 = (m - \Sigma)^2 + p^2 \qquad (6)$$

for a nucleon. In relativistic models without energy or momentum dependent self-energies one obtains

$$m_{\text{eff}} = E - \Sigma_0 = \sqrt{(m^*)^2 + p_F^2} \qquad (7)$$

at the Fermi momentum p_F. The relativistic effective mass (3) cannot be adjusted arbitrarily if a reasonable description of the spin-orbit interaction in atomic nuclei is required. In usual relativistic models we find $m^* \approx 0.55m$ and $m_{\text{eff}} \approx 0.62m > m^*$ at the Fermi momentum but the latter value is rather small. Comparing non-relativistic Skyrme Hartree-Fock calculations for giant resonances in the random phase approximation with experimental data a value $0.78m$ for m_{eff} was extracted [50]. The low Landau mass in conventional RMF models indicates that the level density at the Fermi energy is too small and single-particle levels in finite nuclei are too much spreaded, a well known result of detailed calculations.

Assuming an energy dependence of the self-energies, the effective Landau mass is given by

$$m_{\text{eff}} = (E - \Sigma_0)\left(1 - \frac{d\Sigma_0}{dE}\right) + (m - \Sigma)\frac{d\Sigma}{dE}. \qquad (8)$$

It is clear that the Landau mass can be adjusted more freely if the model allows for energy dependent self energies. However, one can not expect that the density and energy/momentum dependence of the Landau mass as observed, e.g., in DB calculations can be well represented. The result (8) is consistent with the non-relativistic form

$$m_{\text{eff}} = m\left(1 - \frac{dV}{dE}\right) \qquad (9)$$

with an energy-dependent optical potential V taken from (1) in the non-relativistic approximation.

There are attempts to cure the problem of the small Landau mass and the related low density of levels in relativistic models. In Ref. [51] a linear energy dependence of the self-energies was introduced heuristically in an energy window around the Fermi energy in order to increase the effective (Landau) mass and the level density. However, the full self-consistency and the Lorentz invariance of the RMF model are lost. In another approach the Landau mass m_{eff} was increased to the value of $0.76m$ that was necessary to obtain reasonable β decay half-lives [52]. Correspondingly, the Dirac effective mass had to be increased by hand to $m^* = 0.67m$ destroying the usually good description of the spin-orbit splittings in nuclei without additional modifications of the density functional. The authors were able to compensate this reduction of the scalar self-energy by introducing a rather strong tensor interaction in the model but still retaining a reasonable description of other properties.

Considering the above observations it is natural to extend the standard relativistic density functional in a way that energy or momentum dependent self-energies appear in the Kohn-Sham equations. This will be a phenomenological approach introducing new parameters in the model that have to be fitted to properties of nuclear matter and atomic nuclei. In Ref. [53] couplings of the meson fields to derivatives of the nucleon field were introduced in the Lagrangian density with the desired result. In this derivative coupling (DC) model additional densities in the functional appear that were not considered before. It was possible to describe the experimentally observed energy dependence of the optical potential

by adjusting the relevant coupling constants but still retaining reasonable nuclear matter properties. There are, however, some deficiencies of the approach. The density dependence of the momentum dependence was different for scalar and vector self-energies leading to problems in extrapolations of the model to high densities. Since the relativistic energy of the nucleon contains the rest mass rather large contributions of the energy-dependent part of the self-energy are required to show a sizable effect. Simultaneously, a large modification of the standard energy-independent part of the self-energies was required. An attempt to fit the parameters of the model to properties of finite nuclei proved to be very difficult.

Realizing the problems, this paper introduces a modification of the model in Ref. [53] combining the virtues of the density-dependent approach for the coupling constants with the momentum-dependent self-energies. In Sec. II the basic Lagrangian density of the model with density-dependent and derivative couplings (D^{3}C) is introduced and the field equations for nucleons, mesons and the photon are derived. The relevant equations for nucler matter and finite nuclei are presented in Sec. III. The parametrization of the coupling functions and the fit of the parameters to properties of finite nuclei are described in Sec. IV. Results of the model for nuclear matter and finite nuclei are discussed in Sec. V with a comparision to conventional RMF models. Finally, in Sec. VI, conclusions and an outlook complete the paper.

II. LAGRANGIAN DENSITY AND FIELD EQUATIONS

In the present approach the (symmetrized) Lagrangian density assumes the form

$$\mathcal{L} = \frac{1}{2}\left[\bar{\psi}\Gamma_\mu iD^\mu\psi + \overline{(iD^\mu\psi)}\Gamma_\mu\psi\right] - \bar{\psi}\Gamma M^*\psi + \mathcal{L}_m \quad (10)$$

with the nucleon field ψ, the covariant derivative

$$iD_\mu = i\partial_\mu - \Gamma_\omega\omega_\mu - \Gamma_\rho\vec{\tau}\cdot\vec{\rho}_\mu - \Gamma_\gamma\frac{1+\tau_3}{2}A_\mu \quad (11)$$

and the mass operator

$$M^* = m - \Gamma_\sigma\sigma - \Gamma_\delta\vec{\tau}\cdot\vec{\delta}. \quad (12)$$

The meson fields are denoted by σ, ω_μ, $\vec{\delta}$, $\vec{\rho}_\mu$ and the photon field by A_μ. For completeness all four combinations from the alternatives scalar-vector and isoscalar-isovector are included for the mesons. The quantities Γ_σ, Γ_ω, Γ_δ, Γ_ρ and Γ_γ specify the coupling strenght of the mesons and of the photon, respectively, to the nucleon. The elements of the vector $\vec{\tau}$ are the isospin matrices. The contribution

$$\mathcal{L}_m = \frac{1}{2}\left[\partial^\mu\sigma\partial_\mu\sigma - m_\sigma^2\sigma^2 + \partial^\mu\vec{\delta}\cdot\partial_\mu\vec{\delta} - m_\delta^2\vec{\delta}\cdot\vec{\delta}\right. (13)$$
$$\left. -\frac{1}{2}F^{\mu\nu}F_{\mu\nu} - \frac{1}{2}G^{\mu\nu}G_{\mu\nu} + m_\omega^2\omega^\mu\omega_\mu\right.$$

$$\left. -\frac{1}{2}\vec{H}^{\mu\nu}\cdot\vec{H}_{\mu\nu} + m_\rho^2\vec{\rho}^\mu\cdot\vec{\rho}_\mu\right]$$

is the Lagrangian density for the free mesons with masses m_σ, m_ω, m_δ, m_ρ, and the photon with the field tensors

$$F_{\mu\nu} = \partial_\mu A_\nu - \partial_\nu A_\mu \quad (14)$$
$$G_{\mu\nu} = \partial_\mu\omega_\nu - \partial_\nu\omega_\mu \quad (15)$$
$$\vec{H}_{\mu\nu} = \partial_\mu\vec{\rho}_\nu - \partial_\nu\vec{\rho}_\mu. \quad (16)$$

In standard relativistic models the quantities Γ_μ and Γ in Eq. (10) are the Dirac matrices γ_μ and the unit matrix, respectively. In the present approach, they are given by

$$\Gamma_\mu = \gamma^\nu g_{\mu\nu} + \gamma^\nu Y_{\mu\nu} - g_{\mu\nu}Z^\nu \quad (17)$$
$$\Gamma = 1 + \gamma_\mu u_\nu Y^{\mu\nu} - u_\mu Z^\mu \quad (18)$$

with the quantities

$$Y^{\mu\nu} = \frac{\Gamma_V}{m^4}m_\omega^2\omega^\mu\omega^\nu \quad (19)$$
$$Z^\mu = \frac{\Gamma_S}{m^2}\omega^\mu\sigma \quad (20)$$

that depend on the isoscalar σ and ω meson fields. An extension of the approach to isovector fields is obvious. The particular dependence on the meson fields is required by the Lorentz structure in order to generate a linear energy dependence of the scalar and vector self-energies (see below). Furthermore, for both $Y^{\mu\nu}$ and Z^μ a form quadratic in the meson fields was chosen so that the density dependence of the energy dependence is similar for both self-energies in contrast to the DC model [53]. Γ_V and Γ_S represent the two additional couplings of the D^{3}C model that can depend on the nucleon fields similar as the quantities Γ_σ, Γ_ω, Γ_δ, and Γ_ρ in the minimal coupling of the nucleon field to the meson fields. In Eqs. (17) and (18) the metric tensor $g_{\mu\nu} = \text{diag}(1,-1,-1,-1)$ and the four velocity $u_\mu = j_\mu/\varrho_v$ depending on the vector current density $j_\mu = \bar{\psi}\gamma_\mu\psi$ with the vector density $\varrho_v = \sqrt{j_\mu j^\mu}$ appear. Combining the usual minimal meson-nucleon couplings with the action of the quantities Γ_μ and Γ one finds that terms with third powers in the meson fields appear in the Lagrangian like in the non-linear models with meson self interactions. But in the present approach there are no free parameters for these individual terms and they are all accompanied by nuclear fields. Similarly to the standard relativistic models with density-dependent couplings we assume that the couplings Γ_σ, Γ_ω, Γ_δ, and Γ_ρ as well as Γ_V and Γ_S depend on the vector density ϱ_v. In principle, one can also imagine a dependence on other densities, e.g., the scalar density $\varrho_s = \bar{\psi}\psi$. The explicit choice of the functional form will be discussed in Sec. IV.

The Dirac equation, i.e. the Kohn-Sham equation, for the nucleons in the D^{3}C model

$$\gamma^\mu(i\partial_\mu - \Sigma_\mu)\psi - (m - \Sigma)\psi = 0 \quad (21)$$

has the standard form of relativistic models with the vector self-energy

$$\Sigma_\mu = v_\mu - Y_{\mu\nu}\left(iD^\nu - M^*u^\nu\right) + \Sigma_\mu^R \qquad (22)$$

and the scalar self-energy

$$\Sigma = s - Z^\mu\left(iD_\mu - M^*u_\mu\right) \qquad (23)$$

where

$$v_\mu = \Gamma_\omega\omega_\mu + \Gamma_\rho\vec{\tau}\cdot\vec{\rho}_\mu + \Gamma_\gamma\frac{1+\tau_3}{2}A_\mu \qquad (24)$$
$$-\frac{i}{2}\partial^\lambda Y_{\mu\lambda}$$

and

$$s = \Gamma_\sigma\sigma + \Gamma_\delta\vec{\tau}\cdot\vec{\delta} - \frac{i}{2}\partial^\mu Z_\mu \, . \qquad (25)$$

The self-energies in the D^{3}C model are differential operators that act on the nucleon field ψ. The momentum dependence enters through the contributions proportional to $(iD_\mu - M^*u_\mu)$. The time component of this expression mimics the kinetic energy $E - m$ when applied to a plane wave in the absence of meson fields. This is in contrast to the DC model where only the iD_μ term appears [53].

The vector self-energy (22) contains the rearrangement contribution

$$\Sigma_\lambda^R = u_\lambda\left[\Gamma'_\omega\omega_\mu J^\mu + \Gamma'_\rho\vec{\rho}_\mu\cdot\vec{J}^\mu - \Gamma'_\sigma\sigma P_s - \Gamma'_\delta\vec{\delta}\cdot\vec{P}_s \right. \quad (26)$$
$$-\left(t^D_{\nu\mu} - u_\nu j^{M^*}_\mu\right)\frac{\Gamma'_V}{\Gamma_V}Y^{\mu\nu} + \left(j^D_\mu - u_\mu\varrho_s^{M^*}\right)\frac{\Gamma'_S}{\Gamma_S}Z^\mu\Bigg]$$
$$+\left(j^{M^*}_\mu Y^{\mu\nu} - \varrho_s^{M^*}Z^\nu\right)\frac{g_{\nu\lambda} - u_\nu u_\lambda}{\varrho_v}$$

with derivatives $\Gamma'_i = d\Gamma_i/d\varrho_v$ ($i = \sigma, \omega, \delta, \rho, V, S$) and densities

$$J_\mu = \bar{\psi}\Gamma_\mu\psi \qquad \vec{J}_\mu = \bar{\psi}\Gamma_\mu\vec{\tau}\psi \qquad (27)$$
$$P_s = \bar{\psi}\Gamma\psi \qquad \vec{P}_s = \bar{\psi}\Gamma\vec{\tau}\psi \qquad (28)$$

that replace the usual vector and scalar densities. Additionally, the densities

$$t^D_{\mu\nu} = \frac{1}{2}\left[\bar{\psi}\gamma_\mu iD_\nu\psi + \overline{(iD_\nu\psi)}\gamma_\mu\psi\right] \qquad (29)$$
$$j^D_\mu = \frac{1}{2}\left[\bar{\psi}iD_\mu\psi + \overline{(iD_\mu\psi)}\psi\right] \qquad (30)$$
$$j^{M^*}_\mu = \bar{\psi}\gamma_\mu M^*\psi \qquad (31)$$
$$\varrho_s^{M^*} = \bar{\psi}M^*\psi \qquad (32)$$

appear in the rearrangement contribution (26). It is slightly more complicated than in the standard density-dependent (DD) models due to the occurence of the terms with $Y_{\mu\nu}$ and Z_μ. It simplifies considerably for stationary systems. The kinetic densities (29) and (30) are different

from the derivatives $iD_\nu j_\mu$ and $iD_\mu\varrho_s$ of the vector current j_μ and scalar density ϱ_s. The former do not vanish in homogeneous nuclear matter and give a finite contribution.

From the Dirac equation (21) the continuity equations

$$\partial^\mu J_\mu = 0 \quad \text{and} \quad \partial^\mu\vec{J}_\mu = 0 \qquad (33)$$

are derived. Correspondingly, J_0 and $\vec{J}_0$ are the conserved isoscalar and isovector baryon densities instead of $j_0 = \varrho_v$ and $\vec{j}_0 = \bar{\psi}\gamma_0\vec{\tau}\psi$ in standard RMF models.

In the D^{3}C model the field equations of the mesons are obtained as

$$\partial_\mu\partial^\mu\sigma + m_\sigma^2\sigma + \tilde{C}_\mu\omega^\mu = \Gamma_\sigma P_s \qquad (34)$$
$$\partial^\nu G_{\nu\mu} + m_\omega^2\omega^\nu C_{\nu\mu} - \tilde{C}_\mu\sigma = \Gamma_\omega J_\mu \qquad (35)$$
$$\partial_\mu\partial^\mu\vec{\delta} + m_\delta^2\vec{\delta} = \Gamma_\delta\vec{P}_s \qquad (36)$$
$$\partial^\nu\vec{H}_{\nu\mu} + m_\rho^2\vec{\varrho}_\mu = \Gamma_\rho\vec{J}_\mu \qquad (37)$$

with

$$C_{\mu\nu} = g_{\mu\nu} + \frac{\Gamma_V}{m^4}\left(t^D_{\mu\nu} + t^D_{\nu\mu} - u_\nu j^{M^*}_\mu - u_\mu j^{M^*}_\nu\right) \quad (38)$$

and

$$\tilde{C}_\mu = \frac{\Gamma_S}{m^2}\left(j^D_\mu - u_\mu\varrho_s^{M^*}\right) \, . \qquad (39)$$

The source terms are given by simple products of the density-dependent coupling functions Γ_σ, Γ_ω, Γ_δ, Γ_ρ, and the densities (27) and (28). For $\Gamma_S \neq 0$ there is a coupling of the equations for the σ and ω field. Explicit terms with Γ_V appear only in the equation for the ω field due to the factor $C_{\mu\nu}$. The field equation of the photon

$$\partial^\nu F_{\nu\mu} = \Gamma_\gamma J_{\gamma\mu} \qquad (40)$$

has the usual form with the conserved charge current density $J_{\gamma\mu} = [J_\mu + (\vec{J}_\mu)_3]/2$.

III. STATIONARY SYSTEMS

The equations of motion for the nucleons, mesons and the photon field simplify considerably if the nuclear system possesses certain symmetries. E.g., in stationary systems the meson fields are independent of time. For nuclear matter and finite nuclei, it suffices to consider only the time-like component of all four-vectors and the third component of the isospin vectors. The conserved baryon density

$$\varrho = J_0 = j_0\left(1 + Y_{00}\right) - \varrho_s Z_0 \qquad (41)$$

depends on the usual vector density $j_0 = \varrho_v$ and the standard scalar density ϱ_s. Similarly, the generalized scalar density is given by the combination

$$P_s = \varrho_s\left(1 - Z_0\right) + j_0 Y_{00} \qquad (42)$$

with the quantities

$$Y_{00} = \frac{\Gamma_V}{m^4} m_\omega^2 \omega_0^2 \qquad (43)$$

and

$$Z_0 = \frac{\Gamma_S}{m^2} \omega_0 \sigma . \qquad (44)$$

Corresponding equations hold for the isovector densities $\vec{\varrho} = \vec{J}_0$ and $\vec{P}_s$. The self-energies in the Dirac equation can be written as

$$\Sigma_0 = V_0 - Y_{00} i \partial^0 \qquad (45)$$

and

$$\Sigma = S - Z_0 i \partial^0 \qquad (46)$$

with

$$V_0 = v_0 + Y_{00} (v_0 + m - s) + \Sigma_0^R \qquad (47)$$

and

$$S = s + Z_0 (v_0 + m - s) \qquad (48)$$

where

$$v_0 = \Gamma_\omega \omega_0 + \Gamma_\rho \vec{\tau} \cdot \vec{\rho}_0 + \Gamma_\gamma \frac{1 + \tau_3}{2} A_0 \qquad (49)$$

and

$$s = \Gamma_\sigma \sigma + \Gamma_\delta \vec{\tau} \cdot \vec{\delta} \qquad (50)$$

with the rearrangement contribution

$$\Sigma_0^R = \left[\Gamma'_\omega \omega_0 J^0 + \Gamma'_\rho \vec{\rho}_0 \cdot \vec{J}^0 - \Gamma'_\sigma \sigma P_s - \Gamma'_\delta \vec{\delta} \cdot \vec{P}_s \right. \quad (51)$$
$$\left. - \left(t_{00}^D - j_0^{M^*} \right) \frac{\Gamma'_V}{\Gamma_V} Y_{00} + \left(j_0^D - \varrho_s^{M^*} \right) \frac{\Gamma'_S}{\Gamma_S} Z_0 \right] .$$

The partial derivative $i \partial^0$ in (45) and (46) gives the single-particle energy E when applied to a single-particle state in nuclear matter or finite nuclei leading to an explicit energy dependence of the self-energies. Note that the potentials v_0, s, V_0, S, and the self-energies Σ_0 and Σ are generally different for protons and neutrons.

A. Nuclear matter

Solutions of the Dirac equation are given by the plane-wave states

$$\psi(\vec{p}, \sigma, \tau) = u(\vec{p}, \sigma, \tau) \exp\left(-i p_\mu x^\mu \right) \qquad (52)$$

for a nucleon with four momentum $p^\mu = (E, \vec{p})$, energy $E > 0$. The positive-energy four-spinor is denoted by $u(\vec{p}, \sigma, \tau)$ with spin and isospin quantum numbers σ and τ, respectively. The energy E_τ of a proton ($\tau = 1$) or neutron ($\tau = -1$) with momentum p is found in the same way as in Ref. [53] by replacing X_{00} with Y_{00}, Y_0 with Z_0, and setting $W = 0$ in the corresponding expressions.. It is given by

$$E_\tau = (1 + Y_{00})^{-1} \qquad (53)$$
$$\times \left[V_{0\tau} + \frac{1}{\sqrt{1 - B^2}} \left(A_\tau B + \sqrt{A_\tau^2 + p^2} \right) \right]$$

with the quantities

$$A_\tau = \frac{m - S_\tau + B V_{0\tau}}{\sqrt{1 - B^2}} \qquad (54)$$

and

$$B = \frac{Z_0}{1 + Y_{00}} . \qquad (55)$$

The energy density ε and the pressure p are calculated from the energy-momentum tensor. We find

$$\varepsilon = \sum_\tau \left(\varrho_\tau^E - \varrho_{s\tau}^M \right) + m P_s \qquad (56)$$
$$+ \Gamma_\omega \omega_0 J_0 + \Gamma_\rho \vec{\rho}_0 \cdot \vec{J}_0 - \Gamma_\sigma \sigma P_s - \Gamma_\delta \vec{\delta} \cdot \vec{P}_s$$
$$- \frac{1}{2} \left[m_\omega^2 \omega_0^2 + m_\rho^2 \vec{\rho}_0^2 - m_\sigma^2 \sigma^2 - m_\delta^2 \vec{\delta}^2 \right]$$

and

$$p = \frac{1}{3} \sum_\tau \left(\varrho_\tau^E - \varrho_{s\tau}^M \right) + \Sigma_{R0} j_0 \qquad (57)$$
$$+ \frac{1}{2} \left[m_\omega^2 \omega_0^2 + m_\rho^2 \vec{\rho}_0^2 - m_\sigma^2 \sigma^2 - m_\delta^2 \vec{\delta}^2 \right] .$$

The densities ϱ_τ^E and $\varrho_{s\tau}^M$ are calculated similarly as in Ref. [53]. They are given by

$$\varrho_\tau^E = \frac{2 A_\tau B I_1^\tau + A_\tau^2 B^2 I_2^\tau + I_3^\tau}{\pi^2 (1 + Y_{00})(1 - B^2)^{3/2}} \qquad (58)$$

and

$$\varrho_{s\tau}^M = \frac{2 A_\tau B I_1^\tau + A_\tau^2 I_2^\tau + B^2 I_3^\tau}{\pi^2 (1 + Y_{00})(1 - B^2)^{3/2}} \qquad (59)$$

with the integrals

$$I_1^\tau = \frac{1}{3} \left(p_\tau^F \right)^3 , \qquad (60)$$

$$I_2^\tau = \frac{1}{2} \left[p_\tau^F E_\tau^F - A_\tau^2 \ln \frac{p_\tau^F + E_\tau^F}{A_\tau} \right] , \qquad (61)$$

$$I_3^\tau = \frac{3}{4} E_\tau^F I_1^\tau + \frac{1}{4} A_\tau^2 I_2^\tau , \qquad (62)$$

c.f. Ref. [53]. The Fermi momentum p_τ^F is determined from $\varrho_\tau = I_1^\tau / \pi^2$ by the proton and neutron densities. The energy $E_\tau^F = \sqrt{A_\tau^2 + (p_\tau^F)^2}$ also depends on the

quantity A_τ. The standard scalar and the vector densities can be expressed as

$$\varrho_{s\tau} = \frac{BI_1^\tau + A_\tau I_2^\tau}{\pi^2(1 + Y_{00})(1 - B^2)^{1/2}}, \quad (63)$$

$$j_{0\tau} = \frac{I_1^\tau + A_\tau B I_2^\tau}{\pi^2(1 + Y_{00})(1 - B^2)^{1/2}}. \quad (64)$$

We also need the kinetic densities

$$t_{00}^D = \frac{\sum_\tau \varrho_\tau^E}{1 + Y_{00}} \quad (65)$$

and

$$j_0^D = \frac{\sum_\tau \varrho_{s\tau}^E}{1 + Y_{00}} \quad (66)$$

with

$$\varrho_{s\tau}^E = \frac{A_\tau(1 + B^2)I_1^\tau + A_\tau^2 B I_2^\tau + B I_3^\tau}{\pi^2(1 + Y_{00})(1 - B^2)^{3/2}} \quad (67)$$

in the field equations of the mesons. In equation (57) for the pressure p a rearrangement contribution appears explicitly. It guarantees that the D^{3}C model is thermodynamically consistent and the Hugenholtz-van Hove theorem [54] holds as in the case of the DC and DD models.

B. Finite nuclei

The densities and fields in the ground state of finite nuclei do not vary with time but they depend on the spatial coordinates. In the Hartree approximation the state of the nucleus is described by a product of single-particle states $|\phi_i\rangle$ with single-particle energies ε_i (including the rest mass m) that are solutions of the Dirac equation. From the nucleon wave functions the various densities are calculated by a summation over the contributions from the individual nucleons. The meson fields are found by solving the corresponding field equations with space-dependent source terms with appropriate boundary conditions.

The energy of an atomic nucleus in the D^{3}C model is given by

$$E = \sum_i w_i \varepsilon_i + \frac{1}{2} \int d^3r \ [(\Gamma_\sigma + 2\Gamma_\sigma' j_0) \sigma P_s \quad (68)$$
$$+ (\Gamma_\delta + 2\Gamma_\delta' j_0) \vec{\delta} \cdot \vec{P}_s - (\Gamma_\omega + 2\Gamma_\omega' j_0) \omega_0 J_0$$
$$- (\Gamma_\rho + 2\Gamma_\rho' j_0) \vec{\rho}_0 \cdot \vec{J}_0 - \Gamma_\gamma A_0 J_{\gamma 0}]$$
$$+ \int d^3r \ \left[\left(t_{00}^D - j_0^{M^*} \right) \left(1 + \frac{\Gamma_V'}{\Gamma_V} j_0 \right) Y_{00} \right.$$
$$\left. - \left(j_0^D - \varrho_s^{M^*} \right) \left(1 + \frac{\Gamma_S'}{\Gamma_S} j_0 \right) Z_0 \right]$$

with single-particle occupation numbers w_i (in the present case without pairing $w_i = 0$ or 1, respectively).

Besides the usual rearrangement contributions due to the density dependence of the nucleon-meson couplings Γ_σ, Γ_δ, Γ_ω, and Γ_ρ, additional terms appear with the fields Y_{00} and Z_0 that contain derivatives of the couplings Γ_V and Γ_S.

Here, we consider only spherical nuclei. The self-consistent calculation of the spherical nuclei was performed in coordinate space in an angular momentum basis with a discretization of the radial coordinate and a mesh spacing of 0.1 fm using similar procedures as in [41]. A correction of the Coulomb field was introduced as in [41]. Because the translational symmetry in the calculation is broken a c.m. correction has to be added to the energy (68). It has been microscopically calculated in the non-relativistic approximation

$$E_{cm} = -\frac{\langle \vec{P}^2 \rangle}{2mA} \quad (69)$$

with the c.m. momentum $\vec{P} = \sum_{i=1}^A \vec{p}_i$ from the single-particle wave functions [55]. Nuclear radii are also corrected for the c.m. motion. In case of the charge distribution, corrections due to the c.m. motion and the formfactors of protons and neutrons are considered in the calculation of the charge formfactor [22, 23].

IV. PARAMETRIZATION

In order to calculate actual properties of nucler matter and atomic nuclei the parameters entering the Lagrangian have to be specified. For the mass of the nucleon, the ω and the ρ meson the conventional values $m = 939$ MeV, $m_\omega = 783$ MeV and $m_\rho = 763$ MeV were used. The mass of the σ meson m_σ is treated as a free parameter. The δ meson is neglected in the present work. Except for the electromagnetic coupling constant Γ_γ, all parameters in the coupling functions Γ_i and the mass of the σ meson m_σ were obtained from a fit to properties of the eight doubly magic spherical nuclei ^{16}O, ^{24}O, ^{40}Ca, ^{48}Ca, ^{56}Ni, ^{100}Sn, ^{132}Sn, ^{208}Pb that include nuclei close to and far from the valley of stability. Other nuclei were not considered because effects due to nucleon pairing have to included explicitly in this case adding more parameters in the fit.

There is no unique and generally accepted strategy for the fitting procedure [56]. In the present χ^2 fit of the parameters experimental data for binding energies, charge radii, diffraction radii, surface thicknesses, and spin-orbit splittings were taken into account [22, 23]. Furthermore, it was required to reproduce the experimental value of 0.20(4) fm for the neutron skin thickness in ^{208}Pb, i.e. the difference $r_n - r_p$ of the neutron and proton rms radii [57]. In total there are 32 experimental data points used in the fit.

For a comparison of the D^{3}C model with standard density-dependent models, a new parametrization for DD models was derived under the same conditions in the fit

as the D^3C model with the same set of nuclei and experimental data. In this fit the nuclear incompressibility was fixed to $K = 240$ MeV as in the original model in Ref. [41] where only nuclear binding energies were considered. A fit without this constraint leads to unacceptably large values of $K \approx 300$ MeV.

The D^3C model with momentum-dependent self-energies contains two additional coupling functions, Γ_V and Γ_S, as compared to usual DD models. They allow to fit additional properties of the nuclear system under consideration. Here, it was required that the optical potential (1) in symmetric nuclear matter at saturation density assumes the value 50 MeV at a nucleon energy of 1 GeV, a value that is typical for Dirac phenomenology [46, 47].

The density dependence of the coupling functions is written as

$$\Gamma_i(\varrho_v) = \Gamma_i(\varrho_{\mathrm{ref}}) f_i(x) \qquad (70)$$

with the coupling constants $\Gamma_i(\varrho_{\mathrm{ref}})$ at a reference density ϱ_{ref} and suitable functions f_i that depend on the ratio

$$x = \frac{\varrho_v}{\varrho_{\mathrm{ref}}} \qquad (71)$$

with the vector density ϱ_v. Note that the vector density in the D^3C model is not identical with the baryon density ϱ. In the DD model the reference density is just the saturation density ϱ_{sat} of symmetric nuclear matter. The reference density in the D^3C model is different from ϱ_{sat} but it corresponds to the vector density ϱ_v determined at saturation of symmetric nuclear matter.

The functional form of $f_i(x)$ for the density dependence of the σ, ω and ρ meson is assumed to be the same as introduced in Ref. [41] and later used in the parametrizations DD-ME1 [42], DD-ME2 [43], and PKDD [34]. For the σ and ω meson it is given by the rational function

$$f_i(x) = a_i \frac{1 + b_i(x + d_i)^2}{1 + c_i(x + d_i)^2} \qquad (72)$$

with constants a_i, b_i, c_i, and d_i. In order to reduce the number of free parameters it is required that the functions f_σ and f_ω obey the conditions $f_\sigma(1) = f_\omega(1) = 1$, $f'_\sigma(0) = f'_\omega(0) = 0$, and $f''_\sigma(1) = f''_\omega(1)$. For the ρ meson a simple exponential law

$$f_\rho(x) = \exp\left[-a_\rho(x - 1)\right] \qquad (73)$$

is assumed with one free parameter a_ρ as in Ref. [41].

In the D^3C model the quantities Y_{00} and Z_0 are responsible for the energy dependence of the self-energies. Assuming constant couplings Γ_V and Γ_S both Y_{00} and Z_0 show an approximate ϱ^2 dependence at low densities ϱ. This suggests to introduce the power law

$$f_i(x) = x^{-a_i} \qquad (74)$$

as the functional form in order to be able to arbitrarily adjust the density dependence of the energy dependence.

TABLE I: Mass of the σ meson m_σ, parameters of the coupling functions and reference density ϱ_{ref} in the DD and D^3C model.

	DD	D^3C
m_σ [MeV]	547.204590	556.986206
$\Gamma_\sigma(\varrho_{\mathrm{ref}})$	10.685257	11.027474
a_σ	1.371545	1.846341
b_σ	0.644063	3.520730
c_σ	1.034552	7.071799
d_σ	0.567627	0.217107
$\Gamma_\omega(\varrho_{\mathrm{ref}})$	13.312280	13.750549
a_ω	1.385567	2.004516
b_ω	0.521724	4.563703
c_ω	0.869983	9.864792
d_ω	0.618991	0.183821
$\Gamma_\rho(\varrho_{\mathrm{ref}})$	3.639023	3.917462
a_ρ	0.4987	0.4220
$\Gamma_V(\varrho_{\mathrm{ref}})$	0.0	302.188656
$\Gamma_S(\varrho_{\mathrm{ref}})$	0.0	-21.632122
ϱ_{ref} [fm^{-3}]	0.148746	0.128941

In this work the parameters a_V and a_S are set to unity because in this case the second integral in the energy (68) of an atomic nucleus does not contribute and the calculation is simplified.

In total there are ten free parameters in the D^3C model and eight in the DD model. Since several of the parameters are strongly correlated [56] it is convenient to perform the fit not directly in all of these parameters directly but to use saturation properties of symmetric nuclear matter (see subsection V A) as independent variables in the fit and convert these quantities to the coupling constants analytically. Considering the conditions for the neutron skin thickness in ^{208}Pb and the optical potential, the minimum of χ^2 has to be found in an eight- (seven-) dimensional parameter space.

V. RESULTS

The actual values of the model parameters as determined in the fit are given in Table I. The main difference between the DD and the D^3C model are the values of the parameters a_i, b_i, c_i, and d_i for $i = \sigma, \omega$ in the functional form of the density dependence (72). This corresponds to a much stronger increase of the σ and ω coupling for $\varrho \to 0$ in the D^3C model as compared to the DD parametrization. The density dependence of the ρ meson, however, is smaller for D^3C than for DD. Obviously, the constants $\Gamma_V(\varrho_{\mathrm{ref}})$ and $\Gamma_S(\varrho_{\mathrm{ref}})$ are non-vanishing only in the D^3C model. Note that Γ_V is more than ten times larger than Γ_S. Correspondingly, the energy dependence of the vector self-energy is much larger than the energy dependence of the scalar self-energy in

TABLE II: Contributions of nuclear properties with assumed uncertainty in the χ^2 fit of the model parameters and total χ^2 in the DD and D^{3}C model.

property	uncertainty	DD	D^{3}C
binding energies	0.2 MeV	225.2	168.4
charge radii	0.01 fm	44.9	32.4
diffraction radii	0.01 fm	74.7	53.3
surface thicknesses	0.005 fm	15.0	23.0
spin-orbit splittings	0.2 MeV	95.4	60.3
total		455.3	337.4

the present parametrization of the D^{3}C model. The negative sign of $\Gamma_S(\varrho_{\rm ref})$ indicates that the scalar self-energy rises weakly with the energy of the nucleon. In contrast the vector self-energy decreases much more strongly. From Dirac phenomenology [46, 47] one would expect that both the scalar and the vector self-energy decrease at larger nucleon energies. However, by calculating the momentum-dependent contributions to the self-energies from the Fock terms considering one-pion exchange (that is not included in conventional RMF models), an opposite energy dependence of the self-energies is expected [58] with an increase of the scalar self-energy and a decrease of the vector self-energy. The result of the D^{3}C model lies between these two cases.

In Table II the contributions to the total χ^2 by the various nuclear properties in the fit of the parameters are given for the DD and D^{3}C model, respectively. In both cases the error in the binding energies contributes approximately one half to the total χ^2. The D^{3}C model gives a better description of all properties except for the surface thickness with a small increase of the corresponding partial χ^2. The total χ^2 of the D^{3}C model is about 27 % smaller than in the DD model. This represents a considerable improvement in the description of the experimental data. More details for finite nuclei will be discussed in subsection V B.

A. Nuclear matter

The equation of state (EOS) of symmetric nuclear matter, i.e. the binding energy per nucleon as a function of the density ϱ, is depicted in Figure 1. The EOS in the D^{3}C model and the DD model are compared to the result for the nonlinear NL3 parametrization [32] that is widely used in RMF calculations with considerable success. All three curves are very similar below a density of approximately 0.2 fm^{-3}. At high densities there is a noticable difference. The parametrization NL3 leads to the stiffest EOS and the DD model has the softest EOS with the D^{3}C curve lying in between.

A more quantitative comparison of the models is provided by examining the characteristic constants in the
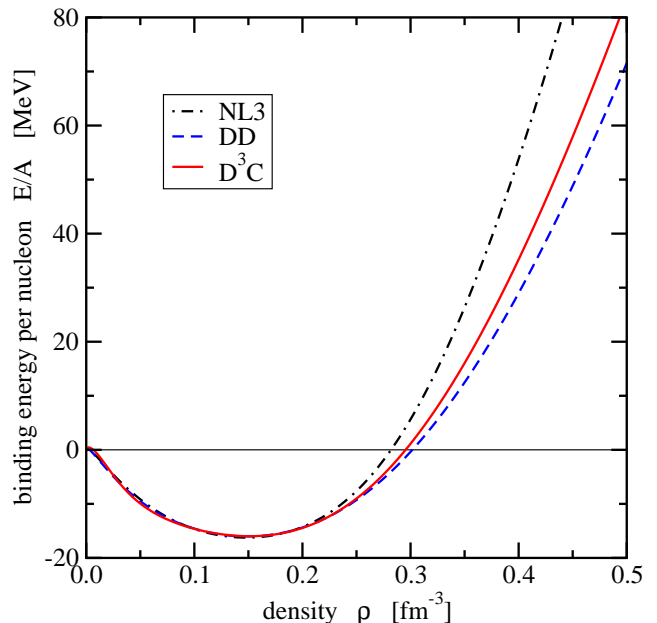

FIG. 1: Equation of state for symmetric nuclear matter in various parametrizations.

expansion of the binding energy per nucleon

$$
\frac{E}{A} = a_V + \frac{K_\infty}{18}\epsilon^2 - \frac{K'}{162}\epsilon^3 + \ldots \qquad (75)
$$
$$
+ \delta^2\left(J + \frac{L}{3}\epsilon + \frac{K_{\rm sym}}{18}\epsilon^2 + \ldots\right)
$$

in nuclear matter near saturation [59, 63]. The deviation of the density from saturation is quantified by

$$
\epsilon = \frac{\varrho - \varrho_{\rm sat}}{\varrho_{\rm sat}} \qquad (76)
$$

and the neutron-proton asymmetry is given by

$$
\delta = \frac{\varrho_n - \varrho_n}{\varrho_n + \varrho_p}. \qquad (77)
$$

In symmetric nuclear matter, i.e. $\delta = 0$, the binding energy at saturation a_V, the incompressibility K_∞, and the derivative K' of the incompressibility determine the form of the EOS. For asymmetric nuclear matter, also the symmetry energy J, the derivative L of the symmetry energy, and the symmetry incompressibility $K_{\rm sym}$ are important. The values of these quantities for the three models NL3, DD, and D^{3}C are given in Table III. A detailed comparison shows that there are major differences between the parametrizations. The D^{3}C model has the softest EOS near saturation (K_∞) but at higher densities is becomes stiffer than the DD model because of the large negative K'. The saturation density is larger than in the DD and NL3 models where the latter model also has a rather strong binding.

TABLE III: Properties of symmetric nuclear matter at saturation in various models.

	NL3	DD	D^{3}C
ϱ_{sat} [fm^{-3}]	0.1482	0.1487	0.1510
a_V [MeV]	-16.240	-16.021	-15.981
K_∞ [MeV]	271.5	240.0	232.5
K' [MeV]	-203.0	-134.6	-716.8
J [MeV]	37.4	31.6	31.9
L [MeV]	118.5	56.0	59.3
K_{sym} [MeV]	100.9	-95.3	-74.7
m^*/m	0.596	0.565	0.541
m_{eff}/m	0.655	0.628	0.710
$V_{\text{cen}}(1\text{ GeV})$ [MeV]	282.2	310.0	50.0
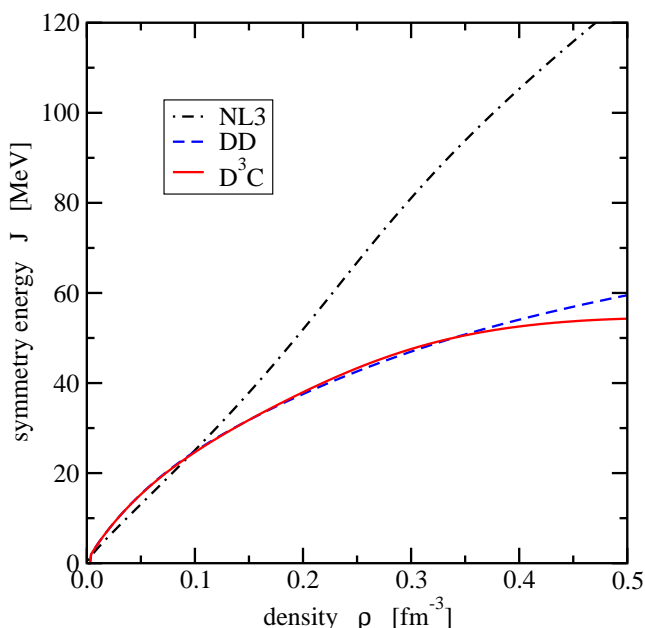
FIG. 2: Symmetry energy J in symmetric nuclear matter as a function of the nucleon density ϱ in various parametrizations.

FIG. 3: Equation of state for neutron matter in various parametrizations.

The symmetry energy J and the derivative L are considerably smaller in the D^{3}C and the DD model than in the NL3 parametrization. This is due to the density dependence of the ρ meson coupling. The actual values are determined by the fit of the neutron skin thickness in ^{208}Pb. The differences in L corresponds to a rather strong deviation in the density dependence of the symmetry energy that is shown in Figure 2. In the NL3 model the symmetry energy rises almost linearly with the density. In contrast, the DD and D^{3}C model exhibit a considerable flattening. This behavior is also reflected in the EOS for neutron matter as presented in Figure 3. Here, the NL3 model shows a very stiff EOS. The shape of the neutron EOS in this model also differs at low densities from the results in the DD and D^{3}C model
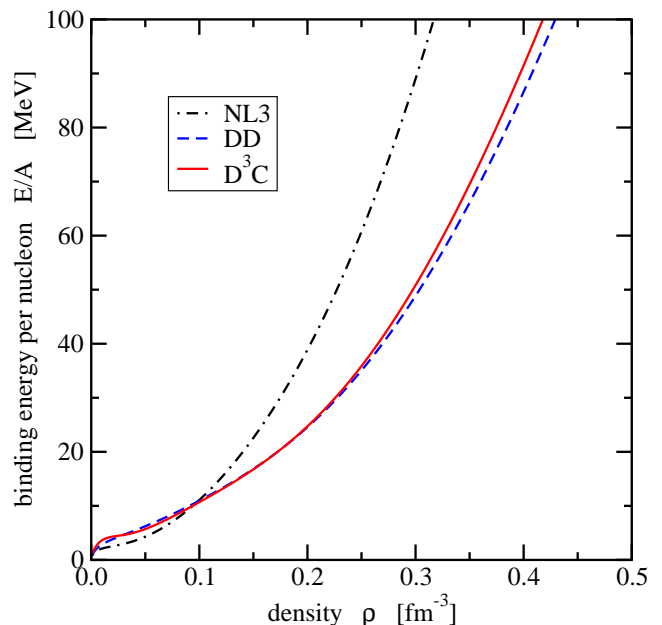
that display very similar results for neutron matter. It is worth noting that the symmetry energy and the neutron EOS in the three models are rather similar at a density near 0.1 fm^{-3}. This value is approximately the neutron density in heavy atomic nuclei. It would be rewarding to study the effects of the different equations of state on the properties of neutron stars but this is beyond the scope of the present work.

Besides the parameters characterizing the EOS, also the Dirac mass m^* and the Landau mass m_{eff} (at the Fermi momentum) are of great interest. The values of these quantities for saturated symmetric nuclear matter are also given in Table III. The D^{3}C model has the smallest value for m^* even below that of the DD model but the Landau mass of 0.710 nucleon masses is the largest of the three models. The χ^2 of the fit is actually not very sensitive to a change in the Landau mass. In principle it is possible to adjust m_{eff} to even larger values at the Fermi surface in saturated symmetric nuclear matter in the D^{3}C model.

The density dependence of m^* and m_{eff} in symmetric nuclear matter is shown in Figure 4. The relativistic effective mass drops strongly with increasing density. At low densities the D^{3}C model is similar to the DD model whereas at high densities it follows more closely the NL3 model. At low densities the Landau mass decreases like the relativistic effective mass with increasing density. However, at higher densities an increase is observed that is easily explained considering the dependence on the Fermi momentum in equations (8) and (7). In the D^{3}C model this increase is very pronounced and the absolute values of m_{eff} are much larger than in the
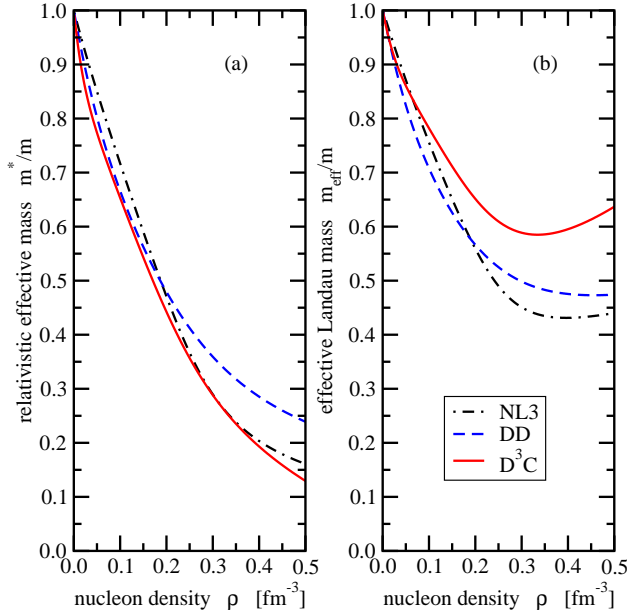
FIG. 4: Relativistic effective mass m^* (a) and effective Landau mass m_{eff} at the Fermi momentum (b) in units of the nucleon mass m in symmetric nuclear matter as a function of the density in various parametrizations.

FIG. 5: Schrödinger-equivalent central optical potential V_{cen} in symmetric nuclear matter as a function of the nucleon kinetic energy $E_{\text{kin}} = E - m$ in various parametrizations and from Dirac phenomenology (DP) of elastic proton-nucleus scattering [46, 47].

other parametrizations that are representative for standard RMF models. Correspondingly, the density of states at the Fermi surface in the D^3C model is considerably higher than that in other RMF models. From the experience in the fitting of the parameters it is found that the requirement of a larger Landau mass at saturation than in the present D^3C model leads to an even softer equation of state for symmetric nuclear matter if one also demands an optical potential of 50 MeV at 1 GeV kinetic nucleon energy. Thus, this last condition should be relaxed in a more extensive parameter fit.

Another major advantage of the D^3C model is the possibility for a very reasonable description of the Schrödinger-equivalent central opical potential as depicted in Figure 5. At low kinetic energies of the nucleon it rises nearly linearly as the empirical optical potential of nuclear matter extracted from Dirac phenomenology for elastic proton-nucleus scattering [46, 47]. At higher nucleon energies it shows a similar saturation with reasonable absolute values. In standard RMF models like NL3 and DD without momentum-dependent self-energies the optical potential rises linearly with the nucleon energy. It approaches unrealistically high values around 300 MeV at 1 GeV kinetic energy (see also Table III). Because the optical potential in the D^3C model is a quadratic function of the nucleon energy, it will ultimately decrease at higher energies und become unrealistic. However, this behavior is not relevant for most applications, e.g. finite nuclei or high-density nuclear matter, because the relevant Fermi momenta and corresponding nucleon energies
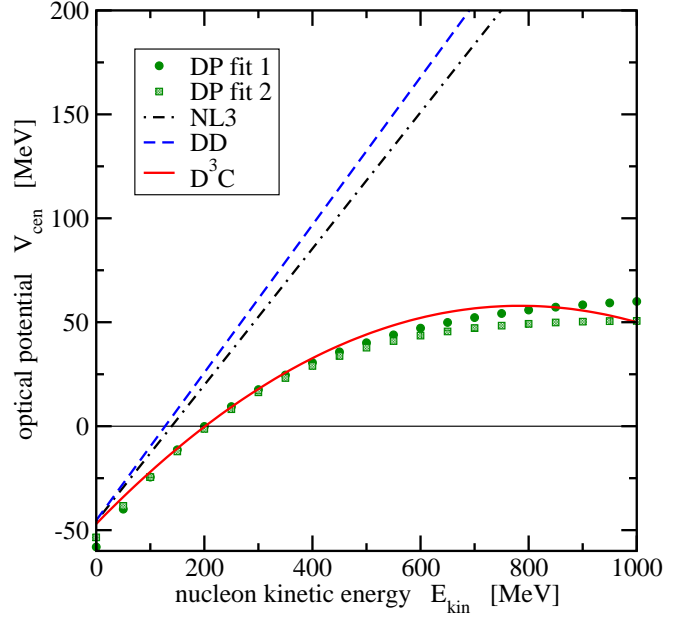
TABLE IV: Total binding energies (in MeV) of the eight fit nuclei in the experiment [64] and in the models DD and D^3C.

Nucleus	Exp.	DD	D^3C
^{16}O	-127.619	-128.064	-127.040
^{24}O	-168.382	-169.114	-169.178
^{40}Ca	-342.052	-342.505	-342.581
^{48}Ca	-415.990	-414.876	-415.047
^{56}Ni	-483.992	-481.924	-482.486
^{100}Sn	-824.794	-826.255	-826.079
^{132}Sn	-1102.851	-1103.359	-1103.478
^{208}Pb	-1636.430	-1636.030	-1635.893

are still small enough in these cases.

B. Finite nuclei

From Table II it was already seen that the D^3C model improves the description of various properties of finite nuclei as compared to the DD model demanding the same conditions in the fit. In Table IV the experimental binding energies [64] of the nuclei that were considered in the fit are compared with the results of the DD and the D^3C model. In general, there is a good reproduction of the experimental data. The absolute root-mean square deviation from the experiment is 1.06 MeV and 0.92 MeV,
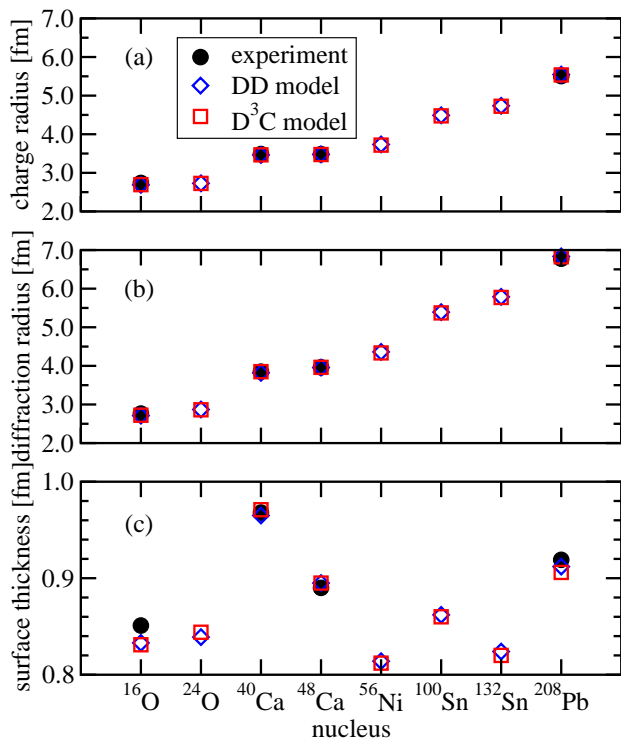
FIG. 6: Charge radius (a), diffraction radius (b), and surface thickness (c) of the fit nuclei in the DD model (blue diamonds) and in the D^3C model (red squares) compared with data from the experiment (solid black dots) [65, 66].

TABLE V: Spin-orbit splitting (in MeV) of neutron (ν) and proton (π) levels in the experiment and in the models DD and D^3C.

Nucleus	State	Exp.	DD	D^3C
^{16}O	$\nu 0p$	6.18	6.761	6.278
	$\pi 0p$	6.32	6.695	6.218
^{48}Ca	$\nu 0f$	8.39	7.961	7.623
	$\nu 1p$	2.03	1.512	1.585
^{56}Ni	$\nu 0f$	7.16	8.568	8.369
	$\nu 1p$	1.12	1.445	1.335
^{132}Sn	$\pi 1d$	1.74	1.996	1.786
	$\pi 0g$	6.09	6.563	6.171
^{208}Pb	$\nu 2p$	0.90	0.917	0.879
	$\pi 1d$	1.33	1.834	1.615
	$\pi 0h$	5.56	6.063	5.642

energies of levels with the same principal quantum number and the same orbital angular momentum. In Table V the results in the DD model and the D^3C model are compared to experimental data for levels close to the Fermi surface. It is found that the spin-orbit splittings of the D^3C model improves the description in most cases when compared to the DD model. This is possible because the relativistic effective mass m^* in the former model is even smaller than in the latter model. At the same time, the Landau mass m_{eff} in the D^3C model is considerably larger than in the DD model. Correspondingly, the level density of the D^3C model is higher. This compression of the spectrum is easily seen when the distribution of single-particle levels is compared for the three heaviest nuclei in the fit in Figure 7. Levels below the Fermi energy are shifted to higher energies and levels above the Fermi energy become more strongly bound.

VI. CONCLUSIONS AND OUTLOOK

In this work the conventional relativistic mean-field model with density-dependent nucleon-meson couplings was extended by introducing a particular form of couplings between the isoscalar meson fields and derivatives of the nucleon fields. This approach leads to a linear momentum dependence of the scalar and vector self-energies in the Dirac equation for the nucleon. The parameters of the model were determined by a fit to properties of finite nuclei. It was possible to improve the description of binding energies, nuclear shapes and spin-orbit splittings of single-particle levels. The characteristic parameters of nuclear matter in the D^3C model are shifted closer to the values of non-relativistic Skyrme Hartree-Fock models [67]. Most noticable was the increase of the effective Landau mass and, correspondingly, the level density at the Fermi surface as compared to standard RMF models. At the same time, the momentum dependence of the
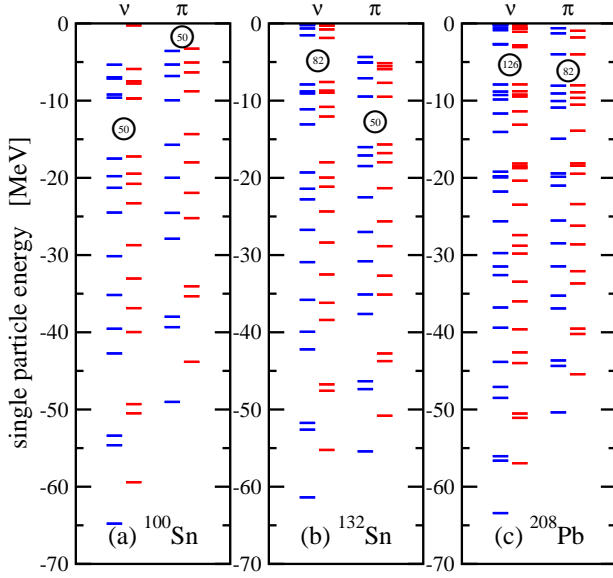
respectively. These values are still larger than corresponding numbers from dedicated fits to masses with rms deviations in the order of a few hundred keV, see, e.g., [60, 61, 62]. For a fair comparison one has to bear in mind that the RMF parametrizations in this work are not just mass models. They are constructed in order to describe a large number of different properties of nuclei and nuclear matter. Furthermore, a valid comparison is only possible when a larger set of (also deformed) nuclei is taken into account. However, this requires a correction for the rotational energy and a reasonable description of pairing effects that is left for future investigations.

The characteristic parameters of the nuclear shape and of the charge form factor, respectively, i.e. the charge radius, the diffraction radius, and the surface thickness [22, 23], are compared to experimental data [65, 66] in Figure 6. Both the DD model and the D^3C model agree very well with the available experimental data. At the same time the difference between the models is very small. They show the same trend for the radii and for the surface thickness. The largest deviation from experiment is found for the surface thickness of ^{16}O, a light nucleus that is not expected to be described very well in a mean-field model.

The last quantity that was considered in the fit is the spin-orbit splitting of proton and neutron single-particle

FIG. 7: Neutron (ν) and proton (π) single particle energies for (a) ^{100}Sn, (b) ^{132}Sn, and (c) ^{208}Pb in the DD (blue lines, left) and D^{3}C (red lines, right) model. The position of the shell closure is denoted by open circles.

self-energies leads to a Schrödinger-equivalent optical potential in symmetric nuclear matter that follows closely the empirical data whereas standard RMF models fail.

The introduction of couplings of the meson fields to derivaties of the nucleon field is a purely phenomenological approach. The goal was to investige possible extensions of the RMF model and their effect on various quantities in nuclear matter and finite nuclei. The origin or the underlying mechanism of the additional couplings is not really relevant in the present context. They are seen only as an effective way to introduce some desired effects in the spirit of density-functional theory. This approach can be compared with the medium dependence that can be parametrized in relativistic mean field models by self-interactions of the meson fields in non-linear models, by density dependent couplings, or even by density dependent meson masses. These approaches are more or less

equivalent when the final results for properties of nuclei are compared, however the underlying mechanisms are quite different.

In principle, of course, one could go beyond the mean field model and discuss in a systematic diagrammatic expansion modifications of the self energies. But this was not the topic of the work. In the present paper, I wanted to stay on a purely phenemenological level in a simple self-consistent approach that has all the necessary features that make it possible to apply the model in practical calculations with reasonable effort to nuclear matter and finite nuclei. The results show that the approach works surprisingly well. The modification of the Lagrangian density can be discussed and treated without reference to more fundamental mechanisms that could generate the corresponding terms.

The density dependence of the momentum dependence is determined in the present model by the choice of the parameters a_V and a_S in Eq. (74). Other values than $a_V = a_S = 1$ as in the present model should be considered. A fit of the model parameters by fixing the Landau mass at the Fermi momentum but varying the absolute value of the Schrödinger-equivalent optical potential is conceivable. The parameter space can be explored more thoroughly allowing for a simultaneous variation of the optical potential and of the Landau mass. The study of deformed nuclei is a further test of the model. However, it will require a larger computational effort and the consideration of pairing effects. It will give more insight into the quality of the description. Applications to neutron stars and to simulations of heavy-ion collisions are also possible. Extensions of the model to introduce an additional isospin dependence of the momentum dependence are obvious.

[1] J. Walecka, Ann. Phys. (N.Y.) **83**, 491 (1974).
[2] B. D. Serot and J. D. Walecka, Adv. Nucl. Phys. **16**, 1 (1986).
[3] P.-G. Reinhard, Rep. Prog. Phys. **52**, 439 (1989).
[4] P. Ring, Prog. Part. Nucl. Phys. **37**, 193 (1996).
[5] J. J. Rusnak and R. J. Furnstahl, Nucl. Phys. **A627**, 495 (1997).
[6] R. M. Dreizler and E. K. U. Gross, *Density Functional Theory*, Springer (1990).
[7] P. Finelli, N. Kaiser, D.. Vretenar, and W. Weise, Nucl. Phys. **A735**, 449 (2004).
[8] P. Hohenberg and W. Kohn, Phys. Rev. **136**, B864 (1964).
[9] W. Kohn and L. J. Sham, Phys. Rev. **140**, A1133 (1965).
[10] J. L. Friar, D. G. Madland, and B. W. Lynn, Phys. Rev. C **53**, 3085 (1996).
[11] R. J. Furnstahl, Brian D. Serot, and Hua-Bin Tang, Nucl. Phys. **A615**, 441 (1997).
[12] L. Sehn, C. Fuchs, and A. Faessler, Phys. Rev. C **56**, 216 (1997)

[13] F. de Jong and H. Lenske, Phys. Rev. C **57**, 3099 (1998).

[14] T. Gross-Boelting, C. Fuchs, and A. Faessler, Nucl. Phys. **A648**, 105 (1999).

[15] F. Hofmann, C. M. Keil, and H. Lenske, Phys. Rev. C **64**, 034314 (2001).

[16] E. N. E. van Dalen, C. Fuchs, and A. Faessler, Nucl. Phys. **A744**, 227 (2004).

[17] B. A. Nikolaus, T. Hoch, and D. G. Madland, Phys. Rev. C **46**, 1757 (1992).

[18] T. Bürvenich, D. G. Madland, J. A. Maruhn, and P.-G. Reinhard, Phys. Rev. C **65**, 044308 (2002).

[19] J. Boguta and A. R. Bodmer, Nucl. Phys. **A292**, 413 (1977).

[20] J. Boguta, Phys. Lett. B **106**, 250 (1981).

[21] J. Boguta and S. A. Moszkowski, Nucl. Phys. **A403**, 445 (1983).

[22] P.-G. Reinhard, M. Rufa, J. Maruhn, W. Greiner, and J. Friedrich, Z. Phys. A **323**, 13 (1986).

[23] M. Rufa, P.-G. Reinhard, J. A. Maruhn, W. Greiner, and M. R. Strayer, Phys. Rev. C **38**, 390 (1988).

[24] P.-G. Reinhard, Z. Phys. A **329**, 257 (1988).

[25] A. R. Bodmer and C. E. Prize, Nucl. Phys. **A505**, 123 (1989).

[26] A. R. Bodmer, Nucl. Phys. **A526**, 703 (1991).

[27] S. Gmuca, J. Phys. G **17**, 1115 (1991); Z. Phys. A **342**, 387 (1992); Nucl. Phys. **A526**, 703 (1992).

[28] M. M. Sharma and P. Ring, Phys. Rev. C **45**, 2514 (1992).

[29] M. M. Sharma, M. A. Nagarajan, and P. Ring, Phys. Lett. B **312**, 377 (1993).

[30] Y. Sugahara and H. Toki, Nucl. Phys. **A579**, 557 (1994).

[31] H. Kouno et al., Phys. Rev. C **52**, 135 (1995).

[32] G. A. Lalazissis, J. König, and P. Ring, Phys. Rev. C **55**, 540 (1997).

[33] H. Toki et al., J. Phys. G **24**, 1479 (1998).

[34] Wenhui Long, Jie Meng, Nguyen Van Giai, and Shan-Gui Zhou, Phys. Rev. C **69**, 034319 (2004).

[35] S. Marcos et al., Phys. Rev. C **39**, 1134 (1989).

[36] L. Sehn and H. H. Wolter, Nucl. Phys. **A519**, 289c (1990).

[37] R. Brockmann and H. Toki, Phys. Rev. Lett. **68**, 3408 (1992).

[38] S. Haddad and M. K. Weigel, Phys. Rev. C **48**, 2740 (1993).

[39] R. Fritz and H. Müther, Phys. Rev. C **49**, 633 (1994).

[40] C. Fuchs, H. Lenske, and H. H. Wolter, Phys. Rev. C **52**, 3043 (1995).

[41] S. Typel and H. H. Wolter, Nucl. Phys. A **656**, 331 (1999).

[42] T. Nikšić, D. Vretenar, P. Finelli, and P. Ring, Phys. Rev. C **66**, 024306 (2002).

[43] G. A. Lalazissis, T. Nikšić, D. Vretenar, and P. Ring, Phys. Rev. C **71**, 024312 (2005).

[44] S. Typel and B. A. Brown, Phys. Rev. C **64**, 027302 (2001).

[45] R. J. Furnstahl, Nucl. Phys. **A706**, 85 (2002).

[46] S. Hama, B. C. Clark, E. D. Cooper, H. S. Sherif, and R. L. Mercer, Phys. Rev. C **41**, 2737 (1990).

[47] E. D. Cooper, S. Hama, B. C. Clark, and R. L. Mercer, Phys. Rev. C **47**, 297 (1993).

[48] S. Typel, O. Riedl, and H. H. Wolter, Nucl. Phys. **A709**, 299 (2002).

[49] M. Jaminon and C. Mahaux, Phys. Rev. C **40**, 354 (1989).

[50] P.-G. Reinhard, Nucl. Phys. **A649**, 305c (1999).

[51] D. Vretenar, T. Nikšić, and P. Ring, Phys. Rev. C **65**, 024321 (2002).

[52] T. Nikšić, T. Marketin, D. Vretenar, N. Paar, and P. Ring, Phys. Rev. C **71**, 014308 (2005).

[53] S. Typel, T. v. Chossy, and H. H. Wolter, Phys. Rev. C **67**, 034002 (2003).

[54] N. M. Hugenholtz and L. van Hove, Physica (Utrecht) **24**, 363 (1958).

[55] M. Bender, K. Rutz, P.-G. Reinhard, and J. A. Maruhn, Eur. Phys. J. A **7**, 467 (2000).

[56] T. J. Bürvenich, D. G. Madland, and P.-G. Reinhard, Nucl. Phys. **A744**, 92 (2004).

[57] V. E. Starodubsky and N. M. Hintz, Phys. Rev. C **49**, 2118 (1994).

[58] T. Maruyama and S. Chiba, Phys. Rev. C **61**, 037301 (2000).

[59] W. D. Myers and W. J. Swiatecki, Ann. Phys. (N.Y.) **55**, 395 (1969).

[60] S. Goriely, F. Tondeur, and J. M. Pearson, At. Data Nucl. Data Tables **77**, 311 (2001).

[61] M. Samyn, S. Goriely, P.-H. Heenen, J. M. Pearson, and E. Tondeur, Nucl. Phys. **A700**, 142 (2002).

[62] D. Lunney, J. M. Pearson, and C. Thibault, Rev. Mod. Phys. **75**, 1021 (2003).

[63] R. C. Nayak, J. M. Pearson, M. Farine, P. Gleissl, and M. Brack, Nucl. Phys. **A516**, 62 (1990).

[64] G. Audi, A. H. Wapstra, and C. Thibault, Nucl. Phys. **A729**, 337 (2003).

[65] C. Fricke, C. Bernhardt, K. Heilig, L. A. Schaller, L. Schellenberg, E. B. Schera, and C. W. de Jager, At. Data Nucl. Data Tables **60**, 177 (1995).

[66] E. G. Nadjakov, K. P. Morrison, and Y. P. Gangrsky, At. Data Nucl. Data Tables **56**, 133 (1994).

[67] M. Bender, P.-H. Heenen, and P.-G. Reinhard, Rev. Mod. Phys. **75**, 121 (2003).